

# A 1D P-wave velocity model of the Gargano promontory (south-eastern Italy)

Salvatore de Lorenzo · Maddalena Michele ·  
Antonio Emolo · Andrea Tallarico

Received: 28 April 2016 / Accepted: 23 January 2017 / Published online: 4 February 2017  
© Springer Science+Business Media Dordrecht 2017

**Abstract** We investigate the elastic properties of the crust in the Gargano promontory, located in the northern part of the Apulia region (Southeastern Italy). Starting on April, 2013, a local-scale seismic network, composed of 12 short-period (1 Hz) seismic stations, was deployed on the Gargano promontory. Starting on October, 2013, the network was integrated with the recordings of nine seismic stations managed by the Italian Institute of Geophysics and Volcanology (INGV). The network recorded more than 1200 seismic events in about 15 months of data acquisition, with more than 700 small magnitude events localized in the Gargano promontory and surrounding areas. A Wadati-modified method allowed us to infer  $V_P/V_S = 1.73$  for the area. A subset of about 400 events having a relatively smaller azimuthal gap ( $<200^\circ$ ) was selected to calibrate a 1D P-wave velocity model of the area, using the VELEST inversion code. The preferred model was obtained from the average of ten velocity models, each of them representing the inversion result from given initial velocity models, calibrated on previous geological and geophysical studies in the area. The results obtained under the assumption that  $V_P$  could decrease with depth are unstable, with very different depths of the top of low-velocity layers. Therefore, the

velocity model was obtained from the average of the results obtained under the assumption that  $V_P$  cannot decrease with depth. A strong reduction of both RMS (about 58%) and errors on the location of the events was obtained with respect to the starting model. The final velocity model shows a strong velocity gradient in the upper 5 km of the crust and a small increase (from 6.7 to 7 km) at 30 km of depth. The epicenters of relocated events do not show clear correlations with the surface projection of known seismic faults. A cluster of the epicenters of the relocated events intersects almost perpendicularly the Candelaro fault trace at the surface.

**Keywords** 1D  $V_P$  velocity model ·  $V_P/V_S$  ratio · Seismic foreland

## 1 Introduction

The Gargano promontory is part of the Adria plate, formed by continental lithosphere and subducting toward west below the Apennine chain; it represents a promontory formed by the collision of Africa and Eurasia plates (Channel et al. 1979). The Adria plate is considered as the foreland of both the Apennines and the southern Alps, at west, and of both the Dinarides and Albanides thrust belts (Fig. 1a), at east (Di Bucci and Angeloni 2013). Several studies (e.g., Tondi et al., 2005) suggest that the Gargano promontory is still not involved in the accretion of central-southern Apennines. In this geodynamic context, the high rate of seismicity, recorded in the last 30 years by the National Seismic

---

S. de Lorenzo (✉) · M. Michele · A. Tallarico  
Dipartimento di Scienze della Terra e Geoambientali, Università di Bari “Aldo Moro”, Bari, Italy  
e-mail: salvatore.delorenzo@uniba.it

A. Emolo  
Dipartimento di Fisica “E. Pancini”, Università degli studi “Federico II”, Naples, Italy

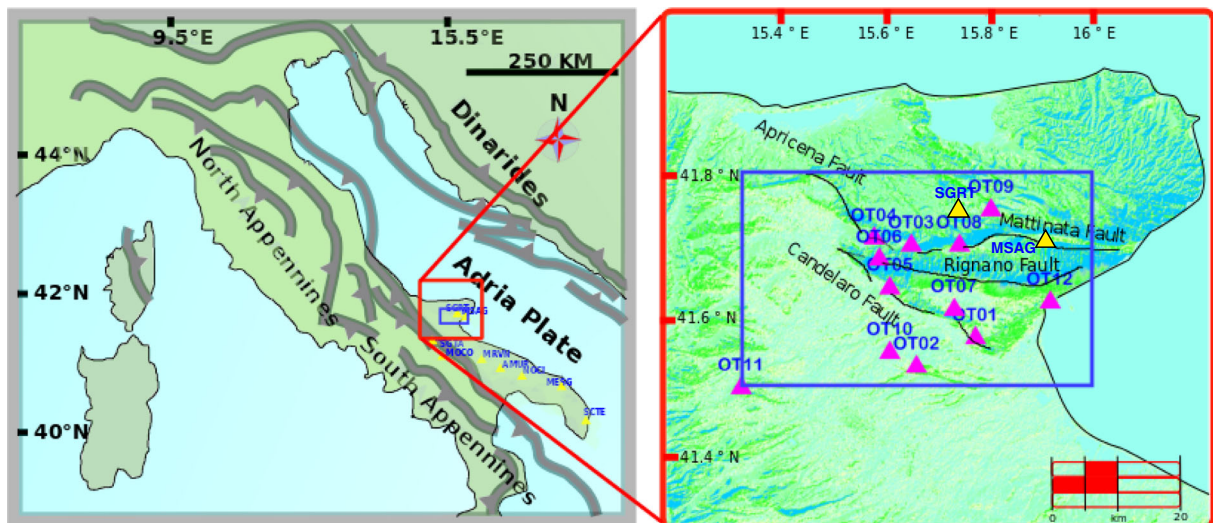


**Fig. 1** **a** Geodynamics of Italy and surrounding areas (Channel et al., 1979). The Adria plate subducts below the Apennine chain toward west and below the Dinarides and Albanides thrust belts toward east. *Yellow triangles* indicate the position of the seismic stations, managed by INGV, considered in this study. **b** The position of the seismic stations (*pink triangles*) of the OTRIONS

network and surface traces of the main faults crosscutting the Gargano promontory. In **a** and **b**, the *red square* encloses the events preliminarily selected for the study; the *blue square* indicates the area enclosing the events used for the inference of the 1D P-wave velocity model

Network (NSN) operated by Italian Institute of Geophysics and Volcanology (INGV), is quite unusual. The most studied seismogenic structure is the Mattinata Fault, a sub-vertical E–W trending fault, which cuts the Gargano plateau for about 45 km (Del Gaudio et al., 2007) (Fig. 1b). This fault has been interpreted as a transfer zone between segments of the chain-foreland system with different kinematics (Doglioni et al. 1994). Other faults, approximately striking in the Apennine direction, have also been considered responsible for the seismic activity of the area. Among these, the most studied are the Apricena fault, responsible of the 1627 earthquake (Patacca and Scandone, 2004) and the Candelaro fault (Fig. 1b), where subvertical movements have been hypothesized (e.g., Billi and Salvini, 2000).

Based on the above argumentations, two questions have to be analyzed: what is the origin of the earthquakes? And, what are the kinematic properties of local faults? To start answering this question, we need to improve the locations of the earthquakes, which also require an improved 1D Earth model. Both these points are the aim of this paper.

On April, 2013, a local-scale seismic network was deployed on the Gargano promontory, located in the northern part of Apulia (south eastern Italy), in the frame of a cooperative experiment between Greek and Italy (acronym OTRIONS), funded by INTERREG programs.

The main aim of the seismic experiment was to reduce the gap of geophysical knowledge in a part of Italy which has been struck by historic earthquakes. In fact, on 30 July 1627, a severe earthquake in this area produced widespread destruction and caused more than 5000 victims (Boschi et al., 1995). At least 11 events, having an estimated  $M_W > 5.5$ , struck the Gargano promontory and surrounding areas in the last millennium (e.g., Del Gaudio et al., 2007).

The inference of an accurate one-dimensional velocity model is the first step in the assessment of the fault structure in a seismogenic area (e.g., Douilly et al., 2013 and references therein), in that it allows precise location of seismic events. In a previous study (de Lorenzo et al., 2014), a regional 1D P-wave velocity model for the Gargano area was inferred by using a mixed dataset of earthquakes, with only few events (about 80) recorded at a local scale. In this paper, we present the first 1D local  $V_P$  velocity model for the Gargano promontory based on a dataset of about 400 earthquakes recorded at a local scale.

## 2 Data

The OTRIONS seismic network was operating since April 23, 2013. It consists of 12 seismic stations

(Fig. 1b), each of them composed of a 24-bit SL06/SARA data-logger (dynamic range equal to 124 dB at 125 sps) equipped with a short-period Lennartz 3D–V seismometer (flat response above 1 Hz). Details on data acquisition and their management are described in de Lorenzo et al. (2014). Data are sampled at 100 sps. Starting on October 23, 2013, the dataset was integrated with seismic data acquired by nine broad-band NSN seismic stations (Fig. 1a). In the period between April 23, 2013 and July, 31, 2014, more than 1360 seismic events were recorded. The arrival times of at least 4 P and 2 S seismic phases were used for the event localization.

A total number of more than 12,789 P-wave arrival times and 11,765 S-wave arrival times were manually picked by expert seismologists with the help of the Seismic Analysis Code (SAC, Goldstein and Snoke, 2005) software, attributing to each of them a weight inversely proportional to their error, following the criterion summarized in Table 1.

These events were initially localized using Hypo71 (Lee and Lahr, 1972) and a 1D P-wave velocity model recently calibrated for the area by de Lorenzo et al. (2014). The location of these events is shown in Fig. 2a. It is evident that about one half of these events occurred on the Gargano promontory and surrounding areas. The local magnitude of these events was computed using the equation recommended by the IASPEI (Bormann and Saul, 2008):

$$M_L = \log_{10}A + 1.11 \log_{10}R + 0.00189 R - 2.09 \quad (1)$$

where  $R$  is the hypocentral distance in kilometers, typically less than 1000 km and  $A$  is the maximum trace amplitude (in nm) measured on the horizontal components of waveforms, after the deconvolution for the instrumental response of the recording seismometer and the convolution with the response of a Wood-

Anderson standard seismograph, but with a static magnification of 1. Equation (1) is the same as that used by INGV for the calculation of the event magnitude and is based on the Hutton and Boore (1987) formulation. For the whole dataset,  $M_L$  ranges from 0 and 6.5 (Fig. 2b). The magnitude distribution of about 700 events recorded on the Gargano promontory and surrounding areas (events enclosed in the red rectangle of Fig. 2a) is shown in Fig. 2c. These events have a magnitude less than 3.1, with the most part of events (80%) having  $M_L$  less than 2 ( $0.3 \leq M_L \leq 1.8$ ).

A total number of 5139 P-wave arrival times ( $T_P$ ) and 4745 S-wave arrival times ( $T_S$ ) was available for the study after the removal of outliers, i.e.,  $T_P$  or  $T_S$  data having a residual higher than 1.5 s with respect to their theoretical value in the initial velocity model.

A modified Wadati diagram was computed for the overall dataset, using the method proposed by Chatelain (1978). It consists of plotting, for each event, the difference  $T_{S,I} - T_{S,J}$ , being  $T_{S,I}$  and  $T_{S,J}$  the S wave arrival times at the  $I$ th and at the  $J$ th stations, respectively, vs. the difference  $T_{P,I} - T_{P,J}$ , being  $T_{P,I}$  and  $T_{P,J}$  the P wave arrival times at the  $I$ th and at the  $J$ th stations, respectively (Fig. 3a). Under the assumption of a homogeneous media, the slope of the straight line that best fits the data furnishes an estimate of the  $V_P/V_S$  ratio. We inferred  $V_P/V_S = 1.73$ . The distribution of  $T_{S,I} - T_{S,J}$  residuals is shown as a function of  $T_{P,I} - T_{P,J}$  in Fig. 3b. The histogram of  $T_{S,I} - T_{S,J}$  residuals (Fig. 3c) indicates that more than 60% of data have an absolute residual less than 0.5 s.

### 3 Method and results

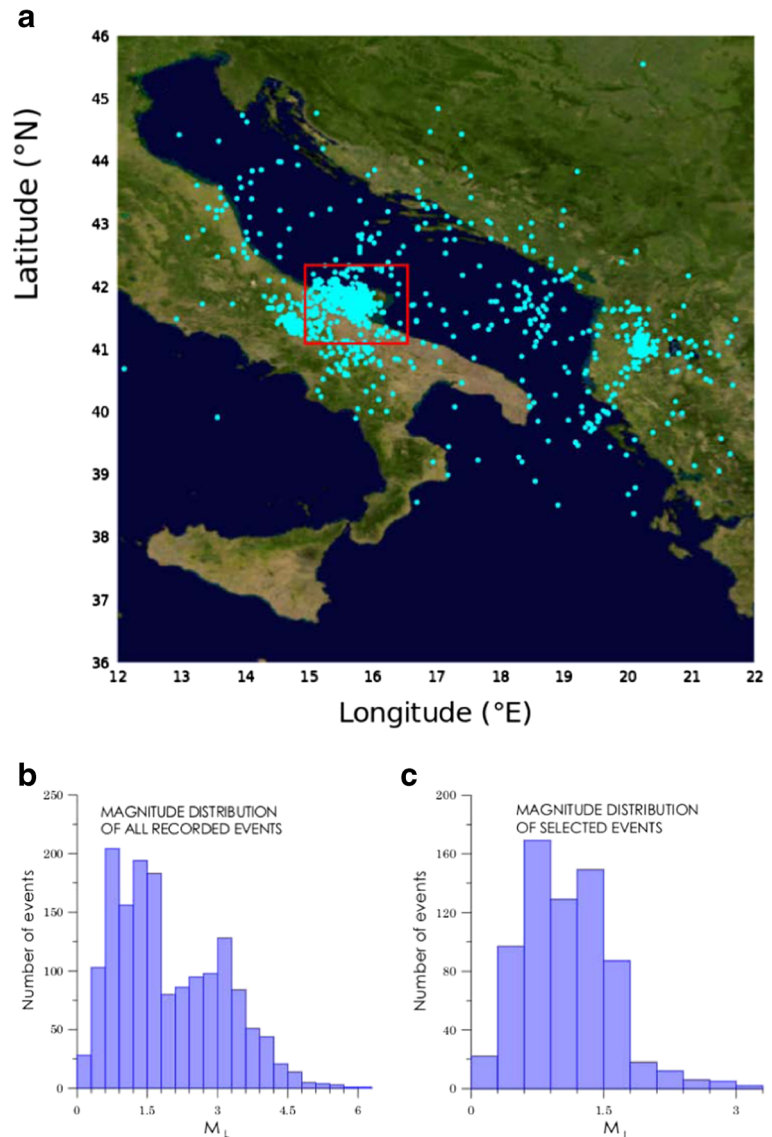
The VELEST (Kissling et al. 1994) inversion code has been used to simultaneously infer the hypocenter parameters and the one-dimensional P-wave velocity model. The inversion is performed through a damped least square inversion scheme, which allows to weight in a different way the hypocenter parameters, the station delays, and the body wave velocity in each layer.

A high number of P- and S-travel time data is generally required to constrain the 1D velocity model and to localize the seismic events (Kissling et al. 1994). Unfortunately, increasing the number of data could increase the error on event localizations, in particular of those events having a higher azimuthal gap, owing to the inclusion in the dataset of some events that are generally located on the outside of the array. In order to obtain a

**Table 1** Weights associated to errors on phase readings

Error (s)	Weight
<0.05	0
(0.05, 0.1)	1
(0.1, 0.2)	2
(0.2, 0.5)	3
>0.5	4

**Fig. 2** **a** The epicenters of all the events recorded at the OTRIONS network using the regional velocity model; the *red square* encloses the events preliminarily selected for the study. **b** The magnitude distribution of all the events. **c** The magnitude distribution of the events enclosed in the *red square* of **a**



reasonable compromise between the need of considering a high number of data and that of minimizing the azimuthal gap, we selected a dataset of about 400 events, whose initial locations are confined in a rectangle having a latitude between  $41.5^\circ$  and  $41.8^\circ$  and a longitude between  $15.3^\circ$  and  $16^\circ$  (the blue rectangle of Fig. 1a, b).

The linearization of the inverse problem causes a dependence of the final result on the initial values of hypocenter parameters and velocity model. This is the reason why a “minimum” 1D velocity model (Kissling et al. 1994) is generally obtained as the average of several retrieved velocity model, each of

them inferred assigning a given initial velocity model.

As a result of several simulation tests, we adopted a two-step iterative inversion scheme. The first step consists in adjusting the hypocenter parameters keeping fixed the  $V_P$  velocity model. In the second step, the velocity model is adjusted by maintaining the hypocenter parameters to the values obtained at the first step. We found out that this is the most efficient way to gain the convergence to the best fit solution, for the actual dataset.  $V_S$  has been computed using the  $V_P/V_S$  ratio inferred in the previous section. In the inversion runs, the  $V_P/V_S$  ratio was fixed to the



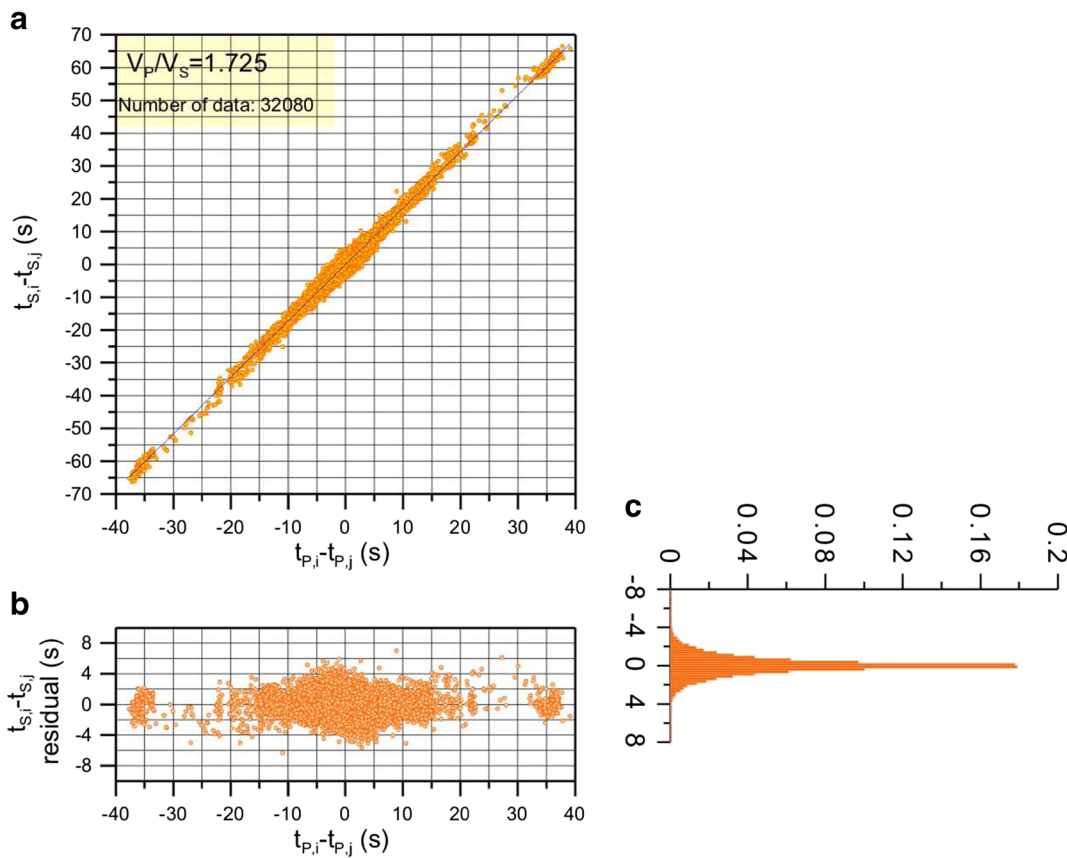


**Fig. 3** **a** Wadati diagram for the entire dataset of 1292 earthquakes considered in this study, **b** plot of  $T_{S_i} - T_{S_j}$  residuals vs.  $T_{P_i} - T_{P_j}$ , **c** Histogram of  $T_{S_i} - T_{S_j}$  residuals

value 1.73, as inferred in the previous paragraph. Even if this value has been determined using the entire dataset, its estimate does not change when considering only local data (red and blue boxes in Fig. 1).

As regards the weighting factors, we followed the guidelines prescribed by Kissling et al. (1994), by using different damping coefficients for hypocenter parameters, station delays, and velocity model. In a first run, we used a damping coefficient equal to 0.01 for hypocenter parameters, a damping coefficient equal to 0.1 for both the station delays and the velocity model. In this step, we jointly inferred source, station, and velocity parameters several times, by updating the starting velocity model with the computed velocity model. After the relocation of the events, we performed a further inversion step, by increasing the damping coefficient for the velocity model to 1, with the aim of finding the velocity model that minimizes the total estimated location error (Kissling et al. 1994). After several trials, we

found out that this is the most efficient scheme to minimize the RMS between observed and theoretical travel times.

As starting velocity models, we adopted ten initial velocity models, shown in Fig. 4a. All these models are derived from preexisting geophysical and geological studies in the area. In particular, the starting homogeneous velocity models and the gradient velocity models (Fig. 4a) have  $V_P$  values comparable with velocity of crustal rocks of the Gargano promontory as inferred in previous studies (Festa et al. 2013). The other initial velocity models (Costa et al., 1993; Venisti et al., 2005; CSTI, 2011; de Lorenzo et al., 2014) arise from previous seismological studies in areas enclosing the Gargano promontory. CSTI, 2001 is the model currently used by INGV in locating the seismic events in the Gargano promontory. The other considered velocity models are based on data recorded in areas that enclose the Gargano promontory; in particular, the velocity

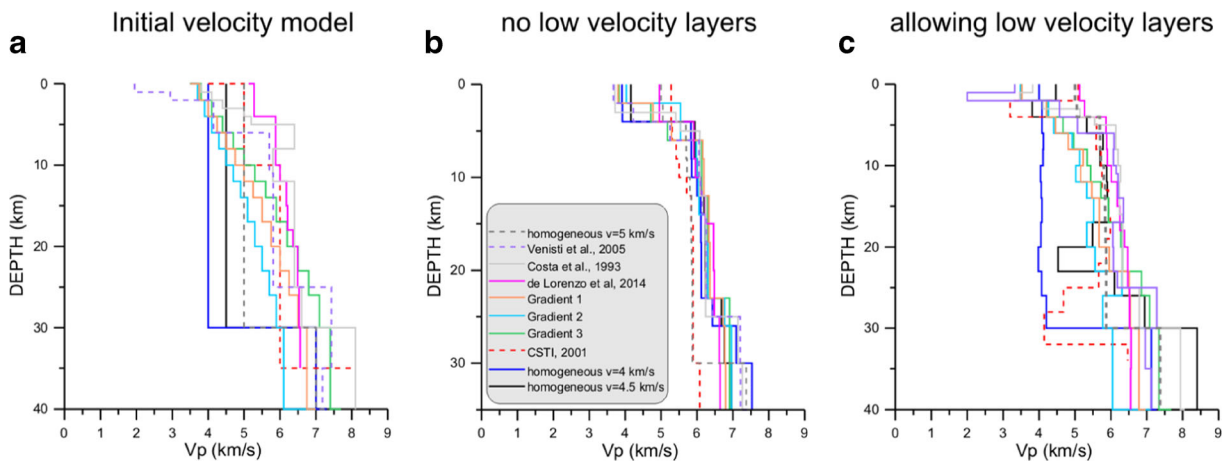


**Fig. 4** **a** Starting velocity models used to infer the 1D P-wave velocity model. VELEST inversion results: **b** excluding low  $V_p$  velocity layers; **c** allowing low  $V_p$  velocity layers

model of Venisti et al. (2005) was used as initial model in a tomographic study of the Adria Plate, whereas the model of Costa et al. (1993) was used in a study of zoning the Gargano promontory in terms of peak ground acceleration; the model of de Lorenzo et al. (2014) has been discussed in the introduction section.

Two different studies have been performed. In a first study, we imposed that  $V_p$  velocity cannot diminish with increasing the depth (Fig. 4b), whereas in a second attempt, we allowed the possibility of a  $V_p$  decrease with the depth (Fig. 4c). As inferred also in previous research papers that use the same approach (e.g., Matrullo et al., 2013), in the latter case, we obtained unstable results. In fact, the inferred velocity models (Fig. 4c) are very different from each other, and this clearly implies their dependence on the initial velocity model and the absence of a convergence toward a minimum 1D model. Moreover, the difference among the results of Fig. 4c concerns also the depth of the low velocity layers, which could reflect in a very different raytracing of P and S waves and therefore in a great variability of the event locations. Finally, the RMS for the case where  $V_p$  velocity cannot diminish with depth is always smaller than the RMS obtained when  $V_p$  is allowed to diminish with depth (Table 2). For this reason, in that follows, we discard the inversion results with low velocity layers.

On the contrary, it is interesting to observe the general similarity of inversion results (with the exception of the CSTI model) under the assumption of the absence of

low velocity layers (Fig. 4b), which indicates a general convergence of the results in this case. As concerns the CSTI model, the difficulty in the convergence may be caused by the presence of a strong velocity contrast at 10 km of depth in the initial model that tend to focus the seismic energy above this depth.

The preferred average 1D velocity model, obtained by averaging the velocity models shown in Fig. 4b, is shown in Fig. 5. The main feature of the inferred velocity model is the strong velocity gradient in the upper 5 km of the crust, where  $V_p$  velocity increases from about 4.3 to about 6.0 km/s, followed by a smaller rate of increase of  $V_p$  with the depth up to 27–30 km of

**Table 2** RMS of the final 1D P-wave velocity models

Velocity model	RMS (s) (no low velocity layers)	RMS (s) (allowing low velocity layers)
De Lorenzo et al. (2014)	0.18	0.20
Venisti et al. (2005)	0.17	0.18
Costa et al. (1993)	0.17	0.18
CSTI (2001)	0.22	0.22
Gradient 1	0.17	0.23
Gradient 2	0.19	0.23
Gradient 3	0.17	0.22
Homogeneous V = 4 KM/S	0.17	0.34
Homogeneous V = 4.5 KM/S	0.17	0.20
Homogeneous V = 5 KM/S	0.19	0.22

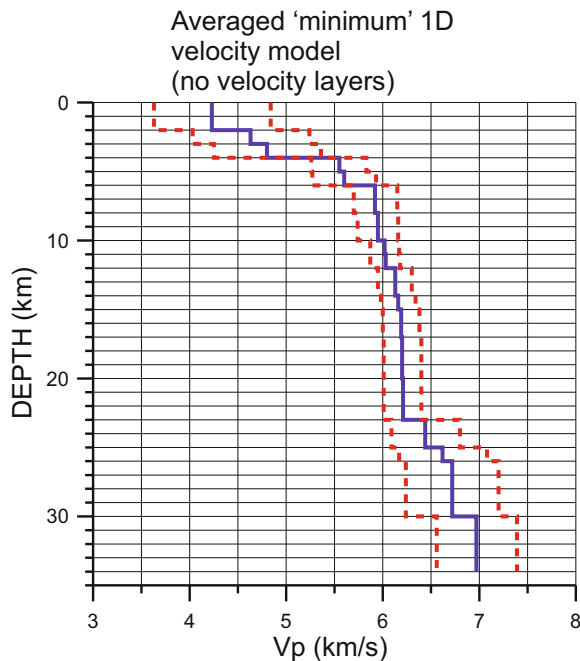


**Fig. 5** Average minimum 1D velocity models (*blue line*) and its error bounds (*red dashed lines*)

depth. A small increase of  $V_p$  at 30 km of depth (from 6.7 to 7 km/s) is also inferred.

The RMS is between 0.17 and 0.19 s for all the ten inverted models (except CSTI), indicating a strong RMS reduction (about 60%) with respect to the value (0.38 s) previously inferred for the mixed dataset (de Lorenzo et al., 2014).

Figure 6a compares the travel time residuals vs. the source-to-receiver distance plots for both the initial model and the final velocity model; the initial model is that considered in the preliminary location of events (de Lorenzo et al., 2014); the final model is the preferred average model shown in Fig. 5. It is worth noting that the initial distribution of residuals is not zero-centered (Fig. 6b), indicating that the initial  $V_p$  model is not well calibrated. This might be caused by the mixed scale (local and regional) of the dataset used in the inference of the previous model (de Lorenzo et al., 2014). This unwanted effect is removed from the use of the 1D  $V_p$  model inferred in this study (Fig. 6c).

A consistent reduction of the average residual in L1 norm (50%), with respect to the preliminary localization, is obtained using the preferred 1D  $V_p$  velocity model. Histograms of travel time residuals

coherently indicate a strong improvement of the results: the percentage of absolute residuals less than 0.1 s increases from 25% in the starting model (Fig. 6b) to 55% in the minimum 1D model (Fig. 6c).

Station delay estimates (Fig. 7) have been obtained by averaging the station delays of the nine inferred velocity models and are generally very small, with the exception of the two stations (MOCO and SGTA) located in the peripheral part of the investigated area. MOCO and SGTA are characterized by relevant site effects (Di Stefano, INGV, personal communication). However, it cannot be ignored that the inferred station residuals at MOCO and SGTA may be also caused by the higher distance of these stations from the region where the most part of events has been located, revealing the existence of uncorrected path effects and therefore deviation of the crustal structure at a regional scale from the local-scale 1D  $V_p$  model inferred in this study.

Earthquakes have been relocated using the preferred average 1D velocity model shown in Fig. 5. Figure 8a compares the epicenters of the sequence and the surface projections of the main seismic faults as inferred in structural geology studies (e.g., Brankman and Aydin, 2004). The highest surface correlation between epicenters and faults is found between a part of the relocated events and the Candelaro horizontal fault trace, letting us to suppose that this structure could be seismically active. Alternatively, another strike-slip fault, almost perpendicular to the Candelaro fault, could explain the location of this cluster of events. This last hypothesis would require further studies based on relative location methods (e.g., Waldhauser and Ellsworth, 2000). Moreover, an approximately north-dipping cluster is inferred from Fig. 8. Also, this problem would benefit of a study based on relative location methods (work in preparation).

However, seismic events do not align with Candelaro fault but tend to cluster in a confined area, in a direction almost perpendicular to its surface projection. Our results seem to indicate an ambiguous relation between the surface trace of the main seismic faults and the position of the epicenters. It seems that seismicity is sparse around the main seismic horizons, confirming the complexity of fault structure in the area hypothesized by Brankman and Aydin (2004).

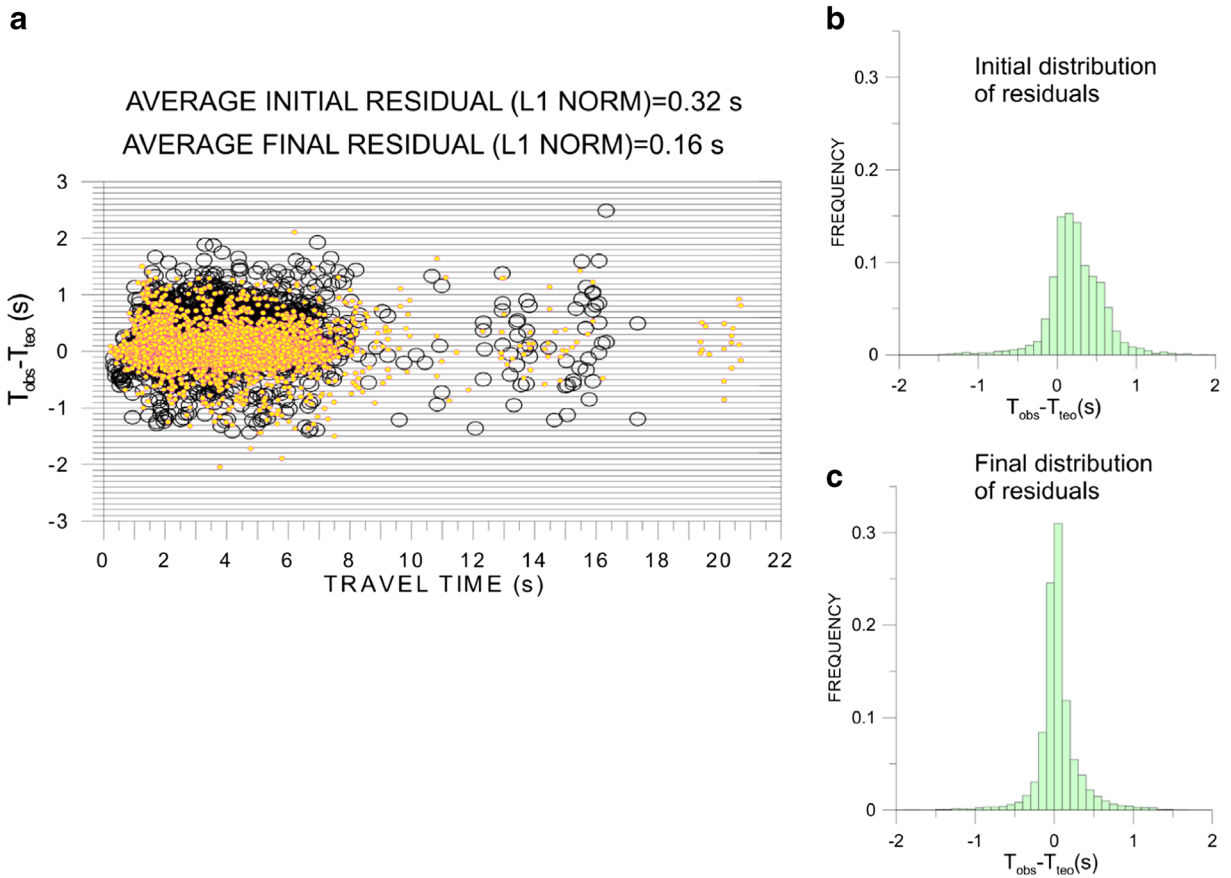
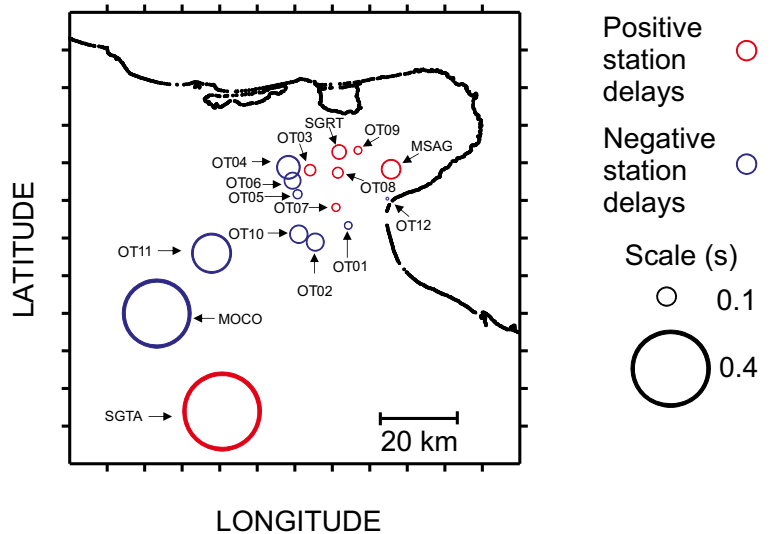


**Fig. 6** Travel time residuals vs. travel times for the initial (*black circles*) and final (*yellow circles*) velocity model. The corresponding histograms of travel time residuals for the initial model (**b**) and the final model (**c**) are also shown

The errors on the horizontal and vertical coordinates of the hypocenters, using the inferred

velocity model, have been computed by relocating the earthquakes with Hypo71 (Lee and Lehr,

**Fig. 7** Station delays inferred in this study. The radius of each circle is proportional to the time scale shown in the inset





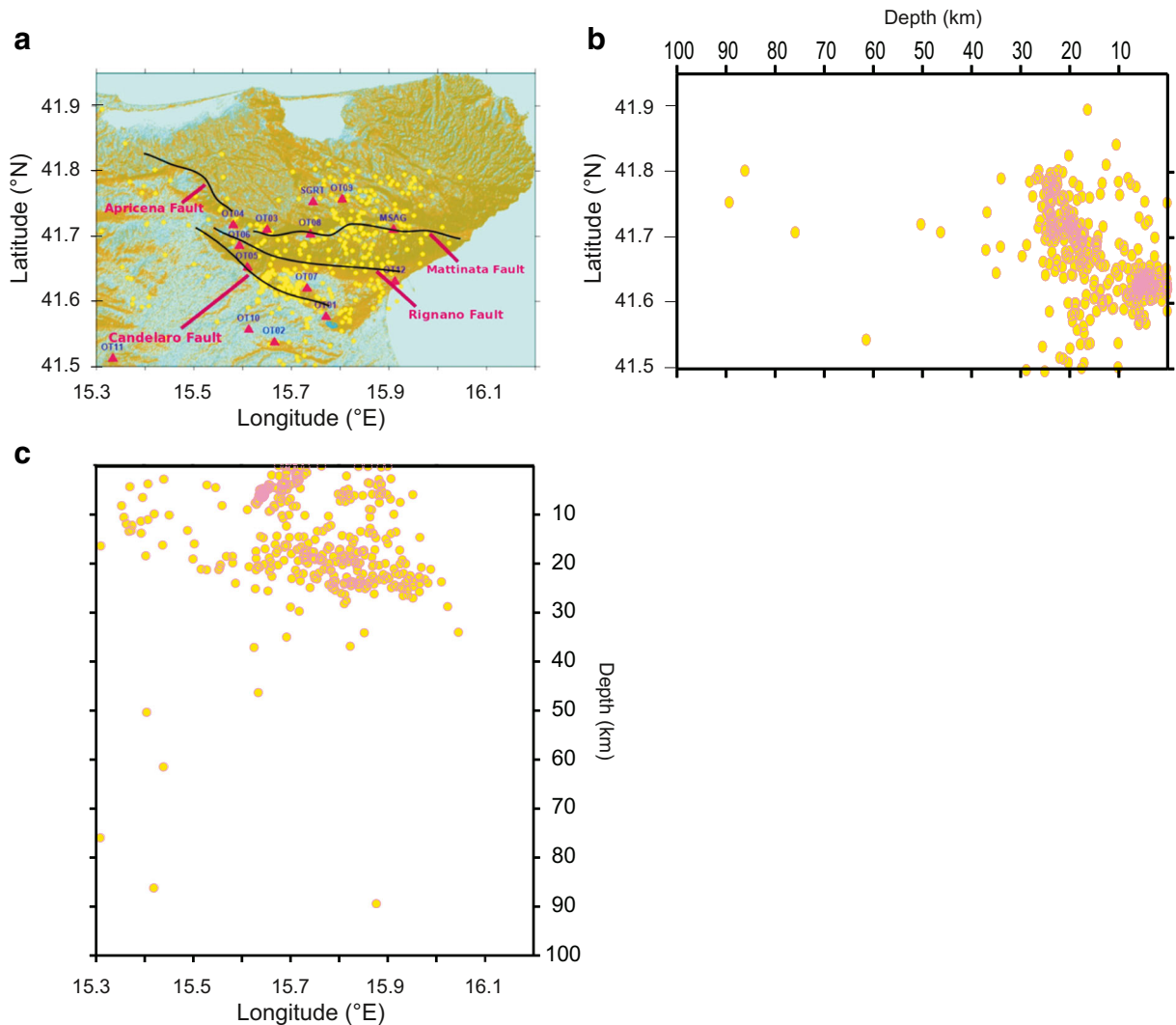


**Fig. 8** Location of the seismic events in the retrieved 1D  $V_p$  velocity model **a** in the horizontal plane, **b** in the latitude-depth plane, **c** in the longitude-depth plane

1972). Figure 9 shows the error maps in the horizontal plane, for both the initial and the minimum 1D velocity model. It is evident the general improving in the location of earthquakes in the minimum 1D model: errors never exceed 10 km almost everywhere, with the exception of few events located in the northwestern part of the considered area, where they are higher owing to the higher azimuthal gap of events. Figure 10 shows the histogram of location errors, for both the starting velocity model and the minimum 1D velocity model: the percentage of events having an error less than 1 km on the horizontal and vertical

coordinate increases from about 45% in the initial model to 75% in the inferred model.

Seismicity is mainly confined above 30 km of the crust. This may imply that Moho should not exceed a depth of 30 km, according to previous conclusions of de Lorenzo et al. (2014) and Piana Agostinetti and Amato (2009). However, the Moho depth is not well constrained, even if a small increase (from 6.7 to 7 km/s) is inferred at 30 km of depth. The small number of events located at a depth greater than 30 km is the main reason for the actual difficulty in constraining the  $V_p$  values below this depth.

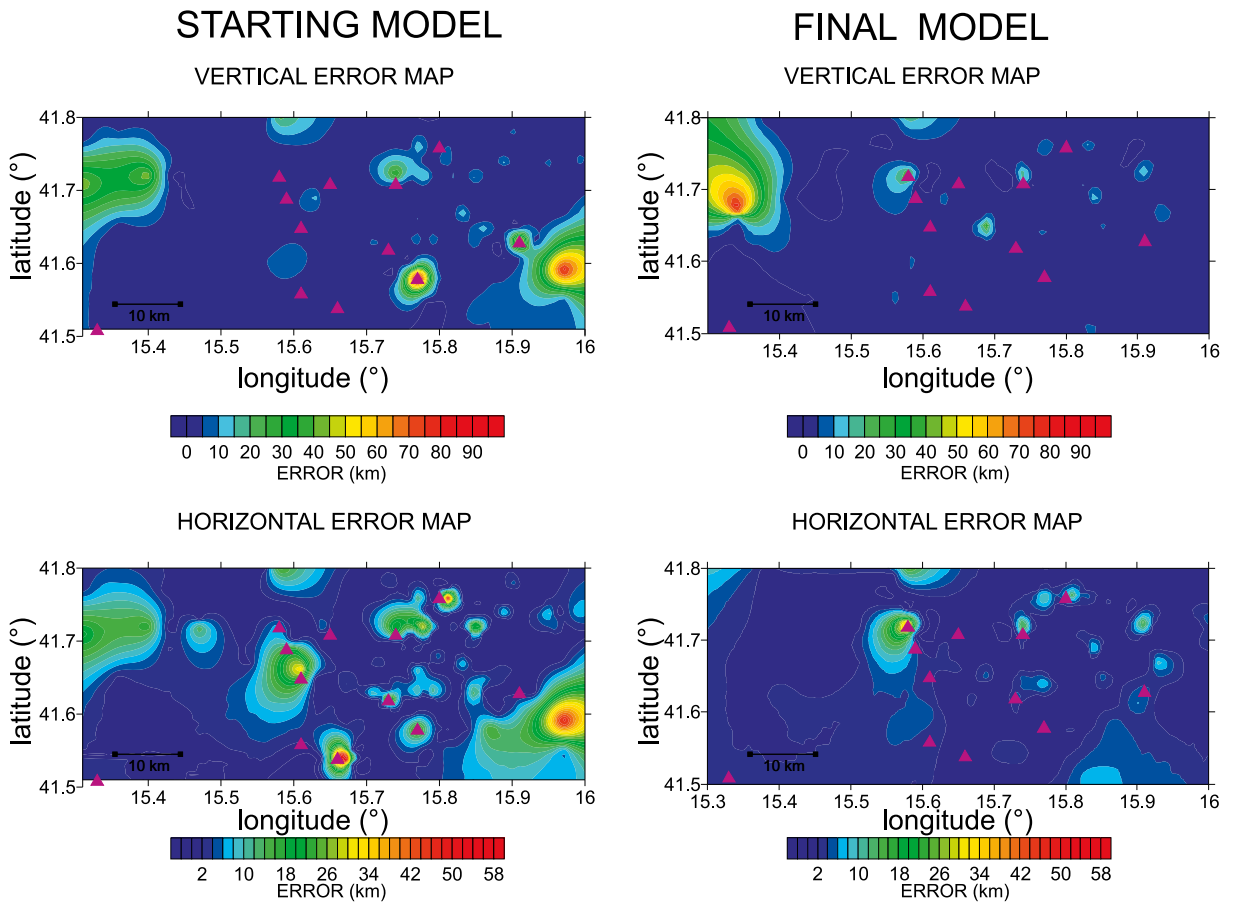


**Fig. 9** Maps of the horizontal and depth errors on localization: **a** for the initial 1D velocity model; **b** for the minimum 1D velocity model

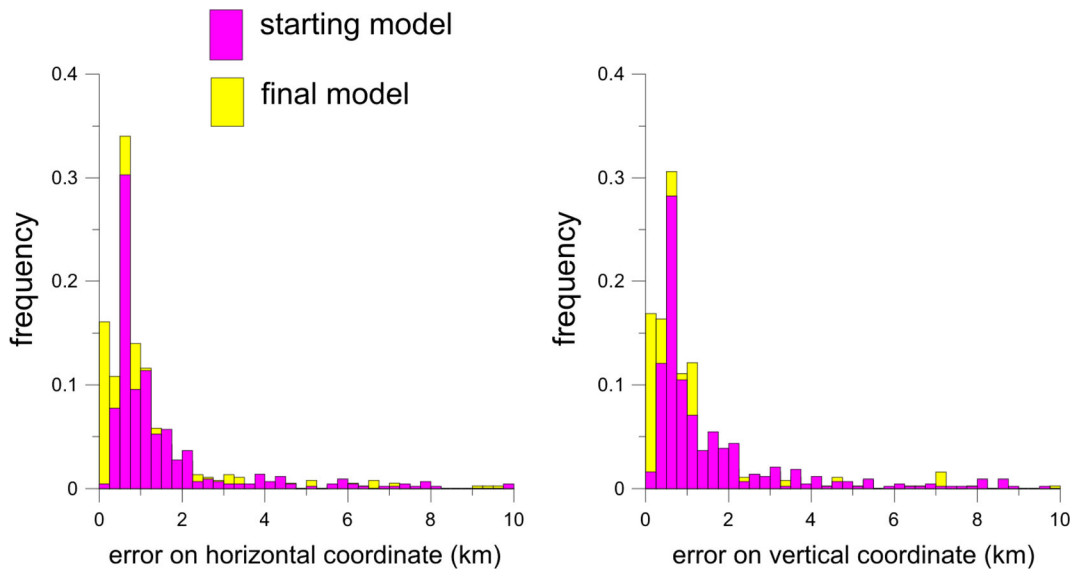


**Fig. 10** Histograms of errors on horizontal and vertical coordinate of hypocenters

## 4 Conclusion

A stable 1D P-wave velocity model for the Gargano area has been inferred from the inversion of P- and S-arrival times of earthquakes recorded at the OTRIONS seismic network. A strong variance reduction has been obtained with respect to the previous model (de Lorenzo et al., 2014) based on mixed (local and regional) datasets.

A strong velocity gradient is found in the initial 5 km of the upper crust, with  $V_P$  that increases from 4.6 km/s at the surface to 6 km/s at 5 km of depth. These features, unexplored in the model of de Lorenzo et al. (2014), indicate that local-scale data are essential to define the local crustal properties with respect to regional models.

The errors on hypocenter coordinates are smaller than those obtained using a mixed dataset (de Lorenzo et al., 2014), indicating that a strong improvement in imaging the seismicity is obtained when using local-scale seismic arrays. However, the geometrical layout of the network has to be improved to reduce the azimuthal gap of many events recorded in the northern part of the Gargano promontory.

A difficult with actual dataset concerns the depth of Moho. In a previous study, Piana Agostinetti and Amato (2009) located the Moho at about 30 km of depth in the Gargano promontory, where a small jump in  $V_P$  velocity (from 6.7 to 7 km/s) is observed. However, since the seismic events are generally located at depths lower than 30 km, the  $V_P$  velocity below this depth is poorly constrained.

Epicenters of events are poorly correlated with surface fault traces, suggesting that a complex fault zone could be responsible for the present activity in the area, as previously hypothesized by Brankman and Aydin (2004). A further 3D tomographic study and/or the use of refined location techniques, based on differential travel time arrivals and a more robust dataset, could help us to better image the fault structure in the area.

## References

- Billi A, Salvini F (2000) Sistemi di fratture associati a faglie in rocce carbonatiche: nuovi dati sull'evoluzione tettonica del Promontorio del Gargano. *Boll. Soc Geol, It* 119:237–250
- Boschi, E., Ferrari, G., Gasperini, P., Guidoboni, E., Smriglio, G. and Valensise, G., 1995, *Catalogo dei forti terremoti in Italia dal 461 a.C. al 1980, ING-SGA*, Bologna, 973 pp.
- Brankman CM, Aydin A (2004) Uplift and contractional deformation along a segmented strike-slip fault system: the Gargano promontory, southern Italy. *J Struct Geol* 26:807–824
- Channel JET, D'Argenio B, Horvath F (1979) Adria, the African promontory, in *Mesozoic Mediterranean palaeogeography*. *Earth Sci Rev* 15:213–292
- Costa G, Panza GF, Suhadolc P, Vaccari F (1993) Zoning of the Italian territory in terms of expected peak ground acceleration derived from complete synthetic seismograms. *J Appl Geophys* 30:149–160
- de Lorenzo, S., Romeo, A., Falco, L., Michele, M., Tallarico, A., (2014) A first look at the Gargano (southern Italy) seismicity as seen by the local scale OTRIONS seismic network, 57, 4, doi:10.4401/ag-6594
- del Gaudio V, Pierri P, Frepoli A, Calcagnile G, Venisti N, Cimini GB (2007) A critical revision of the seismicity of northern Apulia (Adriatic microplate - southern Italy) and implications for the identification of seismogenic structures. *Tectonophysics* 436:9–35
- di Bucci D, Angeloni P (2013) Adria seismicity and seismotectonics: review and critical discussion. *Mar Petrol Geol* 42:182–190
- Dogliani C, Mongelli F, Pieri P (1994) The Puglia uplift (SE Italy): an anomaly in the foreland of the Apenninic subduction due to buckling of a thick continental lithosphere. *Tectonics* 13: 1309–1321
- Douilly R et al (2013) Crustal structure and fault geometry of the 2010 Haiti earthquake from temporary seismometer deployments. *Bull Seism Soc Am* 103:2305–2325. doi:10.1785/0120120303
- Festa V, Teofilo G, Tropeano M, Sabato L, Spalluto L (2013) New insights on diapirism in the Adriatic Sea: the Tremiti salt structure (Apulia offshore, southeastern Italy). *Terra Nova*. doi:10.1111/ter. 12082
- Goldstein P, Snoke A (2005) SAC availability for the IRIS Community. Institutions for Seismology Data Management Center Electronic Newsletter, Incorporated
- Kissling E, Ellsworth WL, Eberhart-Phillips D, Kradolfer U (1994) Initial reference models in local earthquake tomography. *J Geophys Res* 99(B10):19635–19646. doi:10.1029/93JB03138
- Matrullo E, De Matteis R, Satriano C, Amoroso O, Zollo A (2013) An improved 1-D seismic velocity model for seismological studies in the Campania–Lucania region (southern Italy). *Geophys J Int* 195(1):460–473. doi:10.1093/gji/ggt224
- Patacca E, Scandone P (2004) The 1627 Gargano earthquake (southern Italy): identification and characterization of the causative fault. *J Seismol* 8:259–273
- Piana Agostinetti N, Amato A (2009) Moho depth and VP/VS ratio in peninsular Italy from teleseismic receiver functions. *J Geophys Res* 114:B06303. doi:10.1029/2008JB005899
- Tondi E, Piccardi L, Cacon S, Kontny B, Cello G (2005) Structural and time constraints for dextral shear along the seismogenic Mattinata fault (Gargano, southern Italy). *J Geodyn* 40:134–152
- Waldhauser F, Ellsworth WL (2000) A double-difference earthquake location algorithm: method and application to the northern Hayward fault. *Bull Seismol Soc Am* 90:1353–1368